Supporting Information

A 3D Microporous Covalent Organic Framework with exceedingly high C_3H_8/CH_4 and C_2 Hydrocarbons/CH_4 Selectivity

Heping Ma,[a] Hao Ren,*[a] Shuang Meng,[a] Zhuojun Yan,[a] Huanyu Zhao,[a] Fuxing Sun,[a] and Guangshan Zhu*[a,b]

1. Materials and Synthesis

1.1 Materials

All chemcials were purchased from Aldrich, Alfa-Aesar, and Aladdin-reagent, and used as received unless otherwise noted. Actone was dried with anhydrous $CaSO_4$ before used tetra(4-dihydroxyborylphenyl)methane [1] and 1,2,4,5-tetrahydroxybenzene[2] were prepared according to the previously reported method.

References:

[1] J.-H. Fournier, T. Maris, J. D. Wuest, W. Guo, E. Galoppini, *J. Am. Chem. Soc.* 2003，**125**, 1002.

[2] P. W. Weider, L. S. Hegedus, H. Asada, S. V D'Andreq, *J. Org. Chem*. 1985, **50**, 4276.

1.2 Synthesis of the MCOF-1.

Typically, the mixture of TBPM (0.3 mmol) and THB (0.15 mmol) in 1,4-dioxane/mesitylene (1 mL : 0.5 mL) in a sealed Pyrex tube was heated at 90 °C for 3 days. The precipitate was collected by filtration, washed with anhydrous acetone, and dried at 100 °C under vacuum to give COF as a light orange powder in 90% yield.

2. Instruments

FTIR spectra were obtained using an IFS 66V/S Fourier trans-form infrared spectrometer. The thermogravimetric analysis (TGA) was performed using a Netzch Sta 449c thermal analyzer system at the heating rate of 10 °C/min in air atmosphere. Scanning electron microscopy (SEM) imaging was performed on JEOS JSM 6700. The PXRD was performed by a Riguku D/MAX2550 diffractometer using CuKα radiation, 40 kV, 200 mA with scanning rate of 0.3° min-1 (2θ). The^{13}C {^{1}H} CP MAS spectra were recorded on a Bruker AVANCE III 400 WB spectrometer equipped with a 7 mm standard bore CPMAS probehead whose X channel was tuned to 100.62 MHz for ^{13}C and the other channel was tuned to 400.18 MHz for broad band ^{1}H decoupling, using a magnetic field of 9.39T at 297 K. The dried and finely powdered samples were packed in the ZrO_2 rotor closed with Kel-F cap which were spun at 5 kHz rate. The experiments were conducted at a contact time of 2 ms. A total of 5000 scans were recorded with 6 s recycle delay for each sample. All ^{13}C CP MAS chemical shifts are referenced to the resonances of adamantane ($C_{10}H_{16}$) standard (d_{CH2}=38.5). The ^{11}B MAS spectra were recorded on a Bruker AVANCE III 400 WB spectrometer equipped with a 4 mm standard bore CP MAS probehead whose X channel was tuned to 128.39 MHz for ^{11}B, using a magnetic field of 9.39T at 297 K. All^{11}B MAS chemical shifts are referenced to the resonances of boron nitride (BN), 99.5% (metals basis) standard (d=0.00).

Low-pressure gas adsorption measurements:

The gas adsorption/desorption isotherms were measured on a Quantachrome Autosorb iQ2 analyzer. Ar adsorption/desorption measurements were carried out at 87 K. CH_4, C_2H_4, C_2H_6, C_3H_8 adsorption/desorption isotherms collected at 273 K and 298 K, respectively. Ultra-high-purity grade (99.99%) Ar, CH_4, C_2H_6, C_3H_8 and C_2H_4 gases were used for all adsorption measurements. Liquid argon bathe were utilized to control the temperature at 87 K. Ice-water bath and water bathes equipped with a temperature sensor were used to control the temperature at 273 K and 298 K.

3. FT-IR spectra

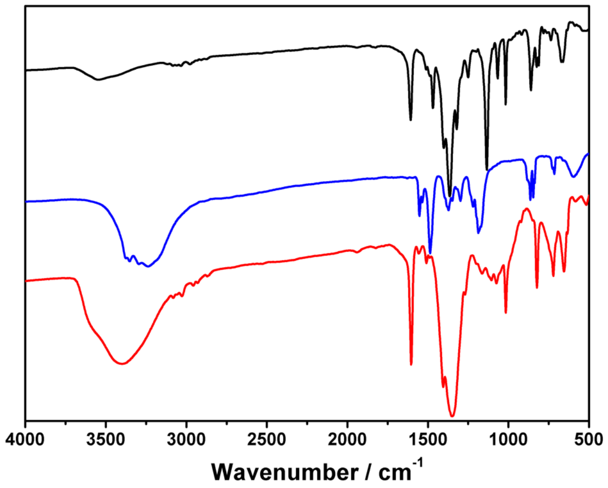

Figure S1. FT-IR spectra of MCOF-1 (black), 1,2,4,5-tetrahydroxybenzene(THB) (blue) and tetra(4-dihydroxyborylphenyl)methane (TBPM) (red).

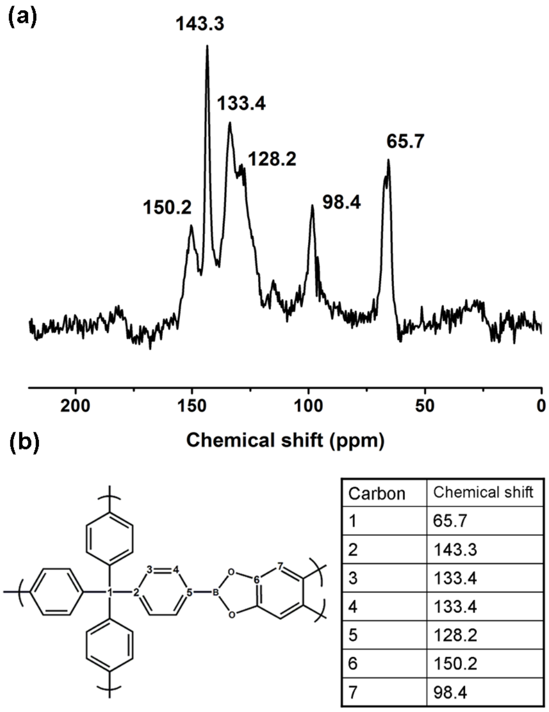

Carbon	Chemical shift
1	65.7
2	143.3
3	133.4
4	133.4
5	128.2
6	150.2
7	98.4

Figure S2. The ^{13}C CP-MAS NMR spectrum of MCOF-1 indicates that the expected building blocks are present.

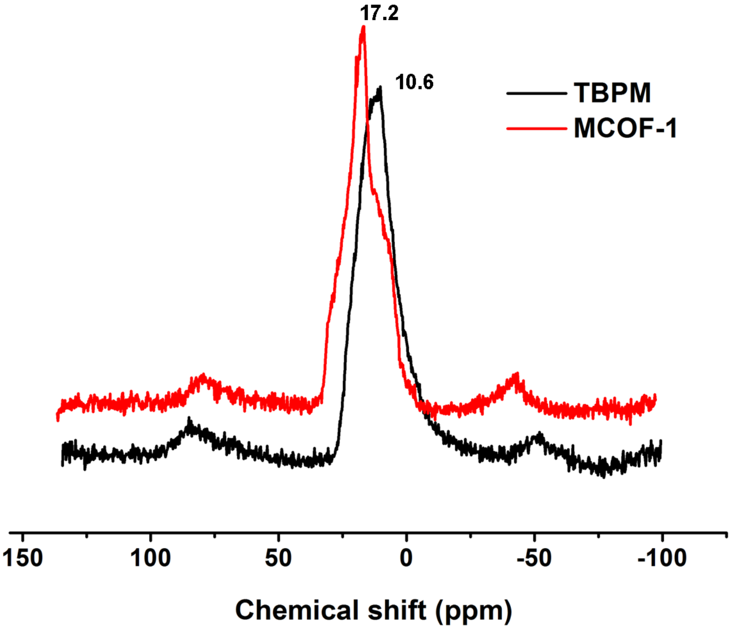

Figure S3. ^{11}B MAS NMR spectrum of MCOF-1 and TBPM.

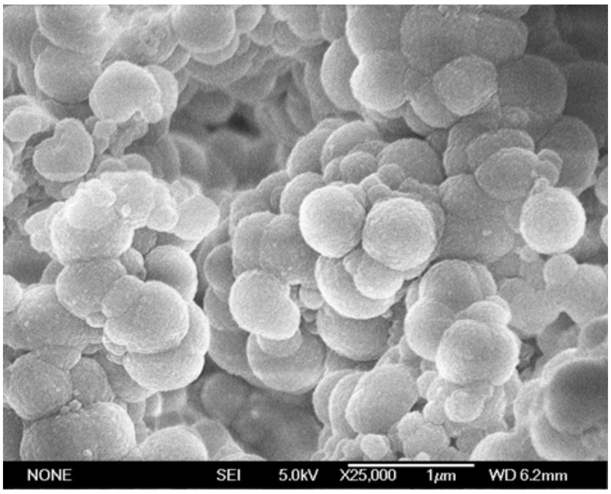

Figure S4. SEM image of MCOF-1 revealing a spherical morphology.

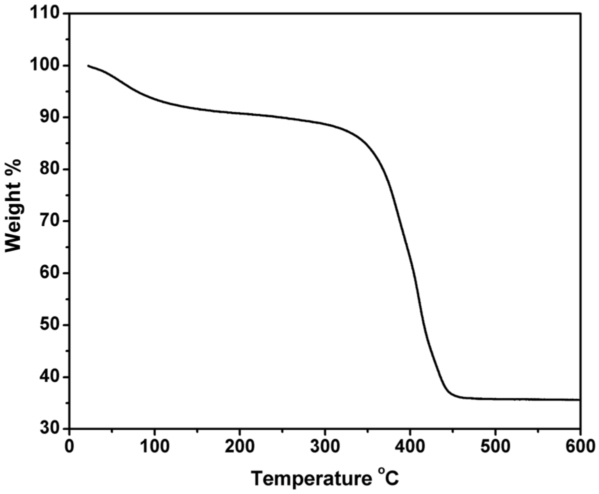

Figure S5. Thermogravimetric analysis of MCOF-1 under air condition.

Structural modelling

All the models, including cell parameters and atomic positions were generated using Accelrys' Materials Studio (MS) v. 4.4 software (Accelrys Software Inc., San Diego, CA, USA) employing the Crystal Building module. Interpenetrative diamond structures were generated using the space groups I4$_1$/a for odd interpenetration, P4$_2$/n for twice odd and P4/n for twice even interpenetration. Vertex positions were obtained from the Reticular Chemistry Structure Resource (http://rcsr.anu.edu.au) under the symbol dia-c3, dia-c4 and dia-c6 for odd, twice even and twice odd respectively. The structures were obtained after replacing all the C—C bonds (edges) with the 2,6-Diphenyl-benzo(1,2-*d*;4,5-*d'*)bis(1,3,2)dioxaborole unit bonding the 4-position of the phenylboronic acid to the tetrahedral carbon. The piecewise structures were minimized with the Forcite module in Materials Studio using the universal force field (UFF). The Simulated PXRD patterns were obtained using the Reflex Powder Diffraction module of Material Studio.

Table S1: Fractional atomic coordinates for dia-c4.

<table>
<tr><td colspan="4">Dia-c4</td></tr>
<tr><td colspan="2">Space Group Symmetry
P4/n
a = b = 19.2868 Å
c = 12.3752 Å
$\alpha = \beta = \gamma = 90^o$</td><td colspan="2">Volume
4603.33 Å^3</td></tr>
<tr><td>Atom</td><td>x</td><td>y</td><td>z</td></tr>
<tr><td>C1</td><td>0.75</td><td>0.25</td><td>0</td></tr>
<tr><td>C2</td><td>0.70591</td><td>0.29477</td><td>0.07775</td></tr>
<tr><td>C3</td><td>0.65331</td><td>0.26289</td><td>0.13982</td></tr>
<tr><td>C4</td><td>0.61530</td><td>0.30046</td><td>0.21590</td></tr>
<tr><td>C5</td><td>0.63015</td><td>0.37048</td><td>0.23441</td></tr>
<tr><td>B1</td><td>0.58793</td><td>0.41243</td><td>0.32015</td></tr>
<tr><td>O1</td><td>0.53171</td><td>0.38194</td><td>0.38417</td></tr>
<tr><td>C6</td><td>0.51253</td><td>0.43876</td><td>0.44564</td></tr>
<tr><td>C7</td><td>0.45973</td><td>0.43984</td><td>0.52332</td></tr>
</table>

Table S2: Fractional atomic coordinates for dia-c5.

Dia-c5			
Space Group Symmetry I 4_1/a a = b = 27.4694 Å c = 9.4034 Å $\alpha = \beta = \gamma = 90^o$		Volume 7051.12 Å^3	
Atom	x	y	z
C1	0	0.75	0.875
C2	0.03783	0.74527	0.73554
C3	0.04823	0.77831	0.60798
C4	0.08460	0.77720	0.49601
C5	0.11054	0.74228	0.50231
B1	0.15374	0.74266	0.39634
O1	0.17025	0.77954	0.29649
C6	0.21078	0.76691	0.26505
C7	0.24195	0.79082	0.17769

Table S3: Fractional atomic coordinates for dia-c6.

Dia-c6			
Space Group Symmetry P42/nnm a = b = 21.200 Å c = 7.0600 Å α = β = γ = 90°		Volume 3173.05 Å^3	
atom	x	y	z
C1	0.75	0.25	0.25
C2	0.70373	0.28371	0.24448
C3	0.65607	0.25601	0.35302
C4	0.61769	0.29345	0.46852
C5	0.62690	0.35900	0.47588
B1	0.58406	0.40100	0.60492
O1	0.53320	0.37524	0.72254
C6	0.51088	0.43009	0.80530
C7	0.46091	0.43403	0.93462

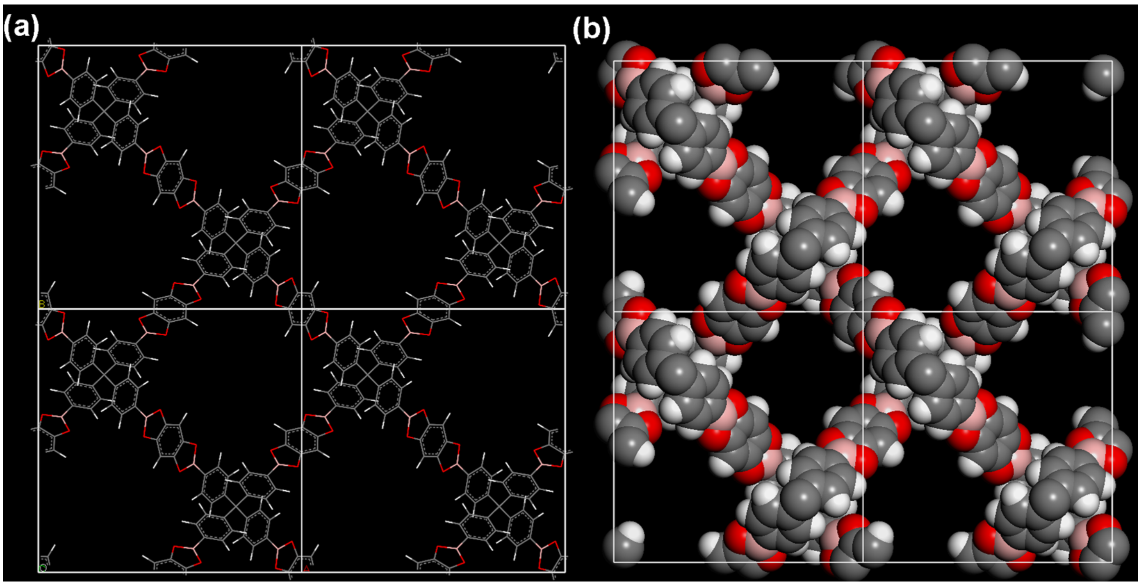

Figure S6: Simulation of crystal structure of dia-c4 in AB plane constructed with 1,2,4,5-tetrahydroxybenzene and tetra(4-dihydroxyborylphenyl)methane.

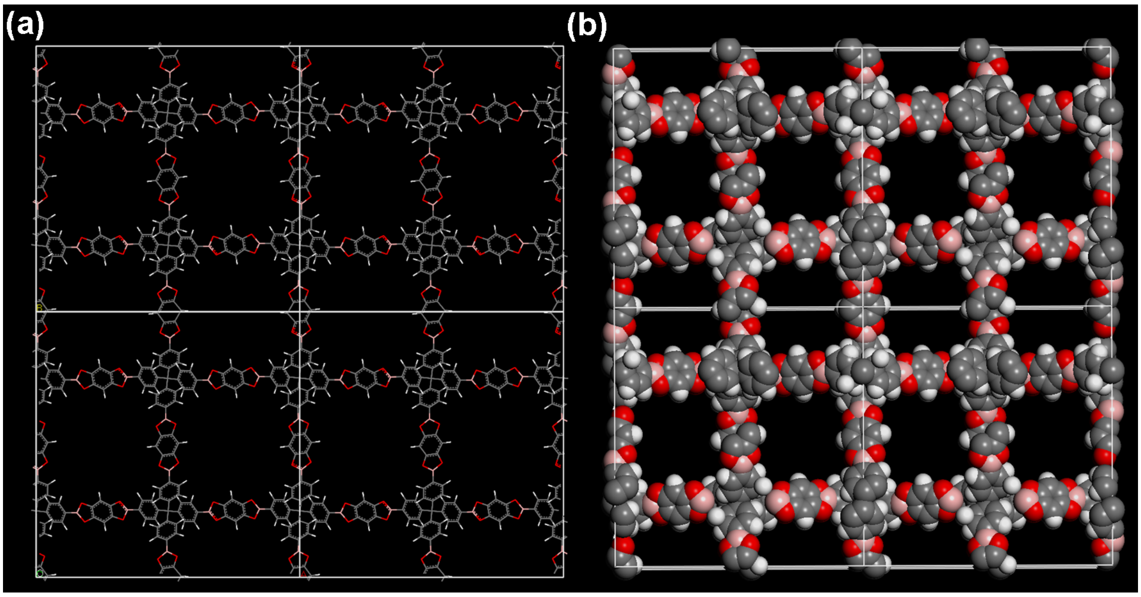

Figure S7: Simulation of crystal structure of dia-c5 in AB plane constructed with 1,2,4,5-tetrahydroxybenzene and tetra(4-dihydroxyborylphenyl)methane.

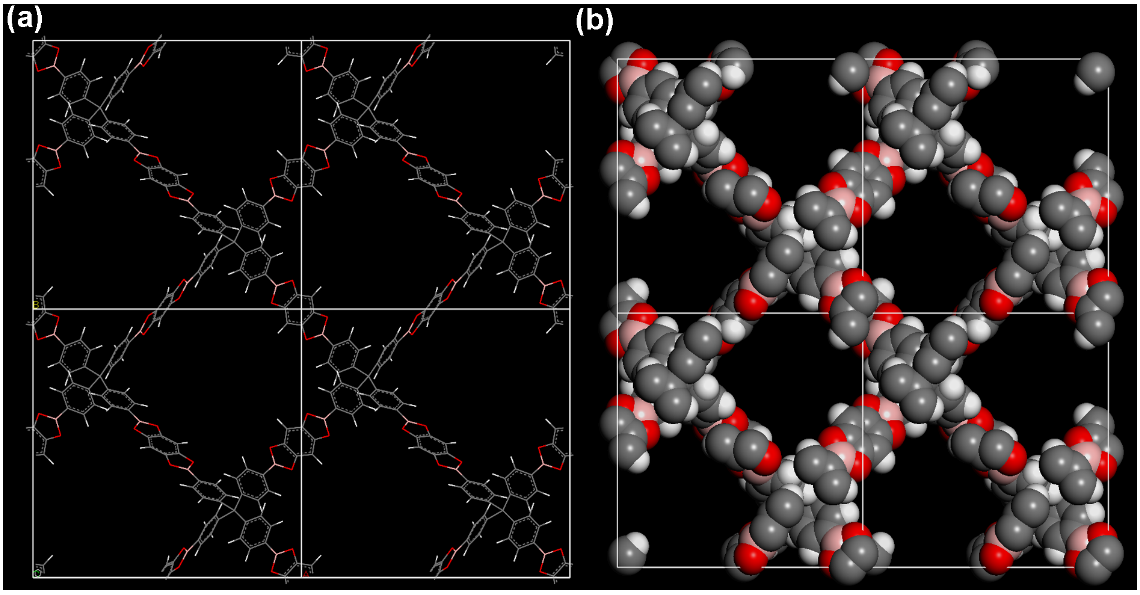

Figure S8: Simulation of crystal structure of dia-c6 in AB plane constructed with 1,2,4,5-tetrahydroxybenzene and tetra(4-dihydroxyborylphenyl)methane.

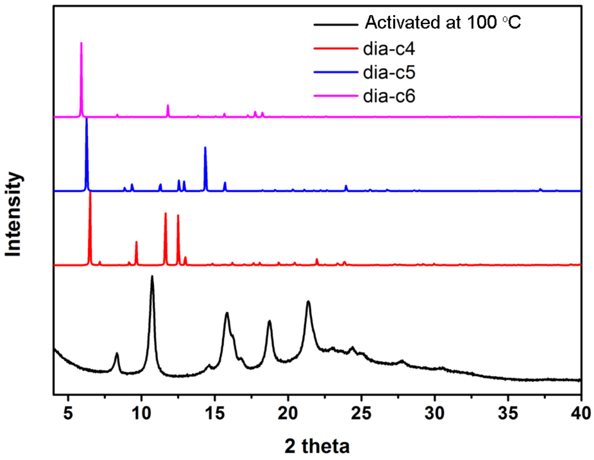

Figure S9. PXRD pattern of MCOF-1 after activated, compared to dia-c4, dia-c5 and dic-c6 simulated pattern.

9. Gas adsorption behavior of MCOF-1 at 273 K.

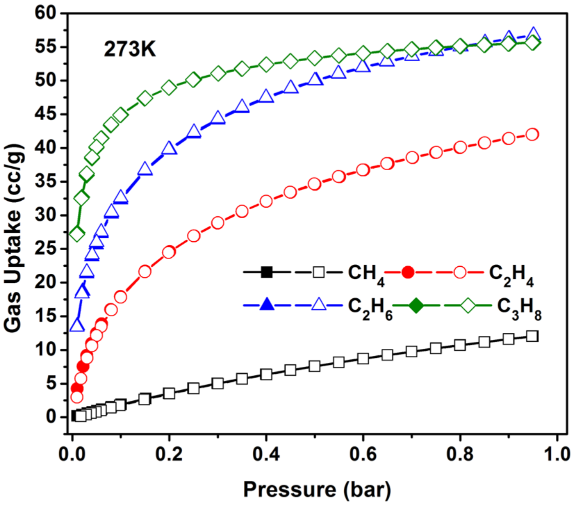

Figure S10. Gas adsorption isotherm for MCOF-1 at 273 K, 1 bar.

10. Isosteric heats of C_2H_4, C_2H_6 and CH_4 for MCOF-1.

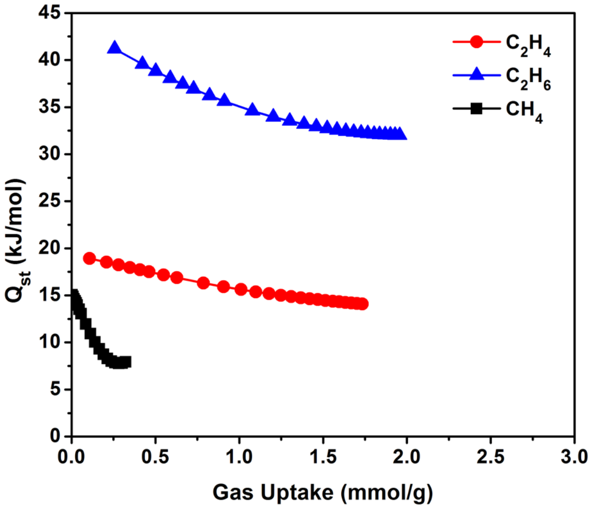

Figure. S11. The isosteric heats of adsorption for MCOF-1 in function of the gas uptake.

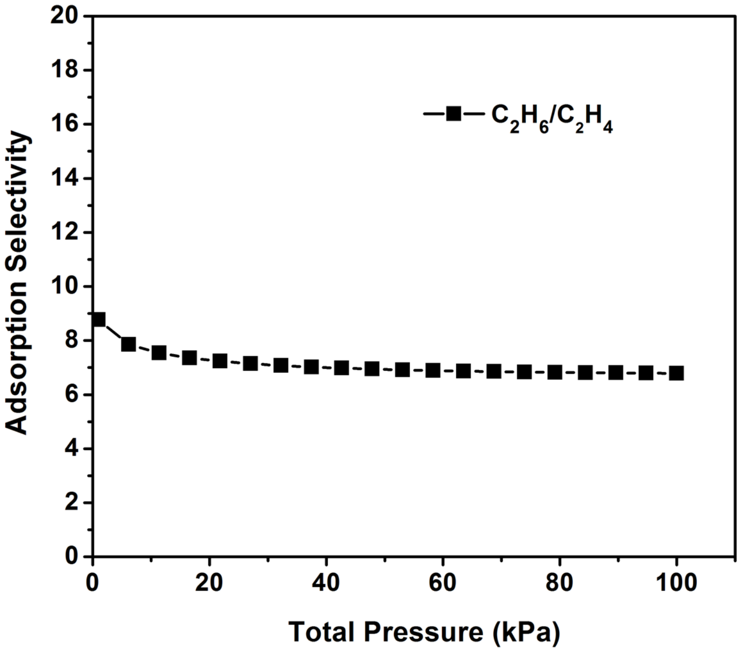

Figure S12. IAST predicted C_2H_6/C_2H_4 equimolar gas mixture adsorption selectivity for MCOF-1 at 273K

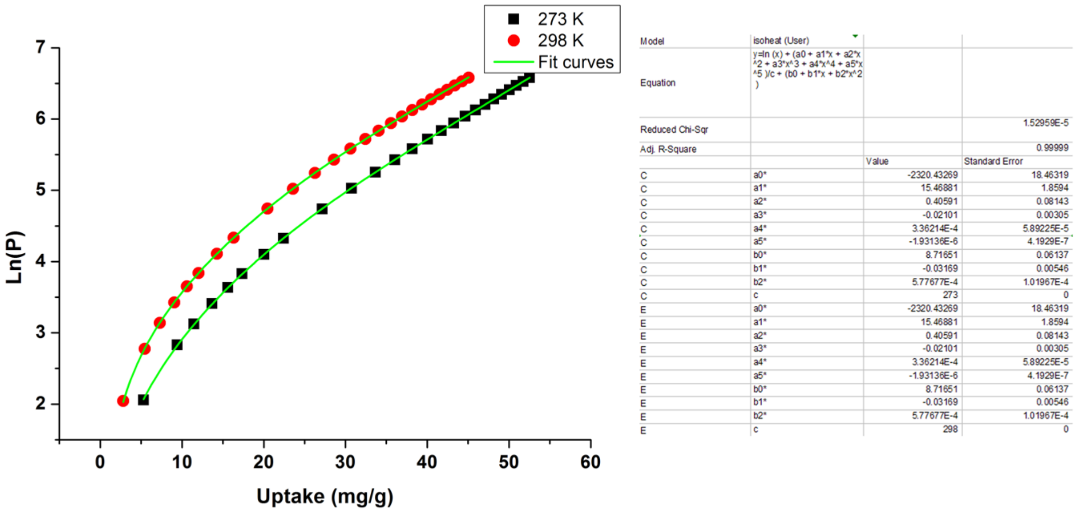

Model	isoheat (User)		
Equation	y=ln (x) + (a0 + a1*x + a2*x^2 + a3*x^3 + a4*x^4 + a5*x^5)/c + (b0 + b1*x + b2*x^2)		
Reduced Chi-Sqr			1.52959E-5
Adj. R-Square			0.99999
		Value	Standard Error
C	a0*	-2320.43269	18.46319
C	a1*	15.46881	1.8594
C	a2*	0.40591	0.08143
C	a3*	-0.02101	0.00305
C	a4*	3.36214E-4	5.89225E-5
C	a5*	-1.93136E-6	4.1929E-7
C	b0*	8.71651	0.06137
C	b1*	-0.03169	0.00546
C	b2*	5.77677E-4	1.01967E-4
C	c	273	0
E	a0*	-2320.43269	18.46319
E	a1*	15.46881	1.8594
E	a2*	0.40591	0.08143
E	a3*	-0.02101	0.00305
E	a4*	3.36214E-4	5.89225E-5
E	a5*	-1.93136E-6	4.1929E-7
E	b0*	8.71651	0.06137
E	b1*	-0.03169	0.00546
E	b2*	5.77677E-4	1.01967E-4
E	c	298	0

Figure S13. Nonlinear curve fitting of C_2H_4 for MCOF-1 at different temperatures.

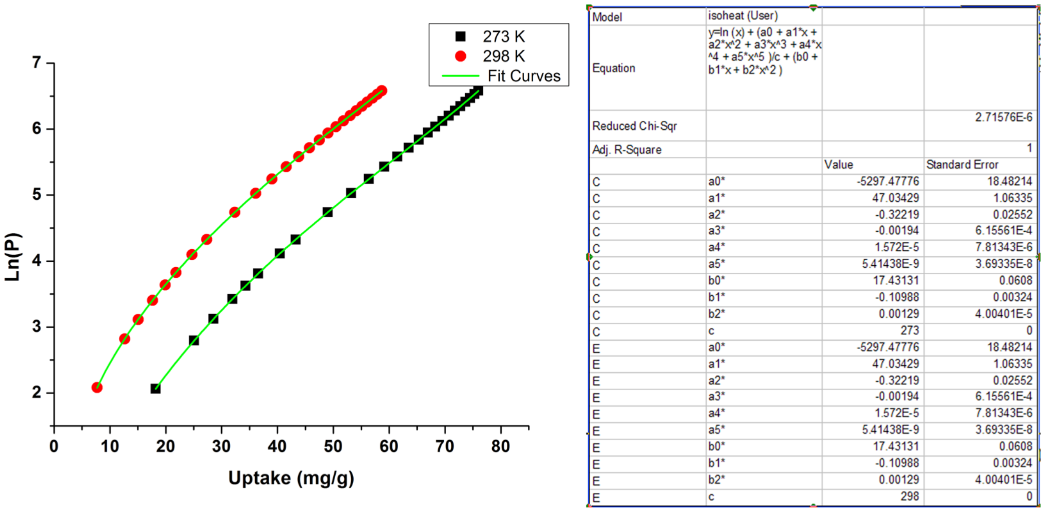

Model	isoheat (User)		
Equation	y=ln (x) + (a0 + a1*x + a2*x^2 + a3*x^3 + a4*x^4 + a5*x^5)/c + (b0 + b1*x + b2*x^2)		
Reduced Chi-Sqr			2.71576E-6
Adj. R-Square			1
		Value	Standard Error
C	a0*	-5297.47776	18.48214
C	a1*	47.03429	1.06335
C	a2*	-0.32219	0.02552
C	a3*	-0.00194	6.15561E-4
C	a4*	1.572E-5	7.81343E-6
C	a5*	5.41438E-9	3.69335E-8
C	b0*	17.43131	0.0608
C	b1*	-0.10988	0.00324
C	b2*	0.00129	4.00401E-5
C	c	273	0
E	a0*	-5297.47776	18.48214
E	a1*	47.03429	1.06335
E	a2*	-0.32219	0.02552
E	a3*	-0.00194	6.15561E-4
E	a4*	1.572E-5	7.81343E-6
E	a5*	5.41438E-9	3.69335E-8
E	b0*	17.43131	0.0608
E	b1*	-0.10988	0.00324
E	b2*	0.00129	4.00401E-5
E	c	298	0

Figure S14. Nonlinear curve fitting of C_2H_6 for MCOF-1 at different temperatures.

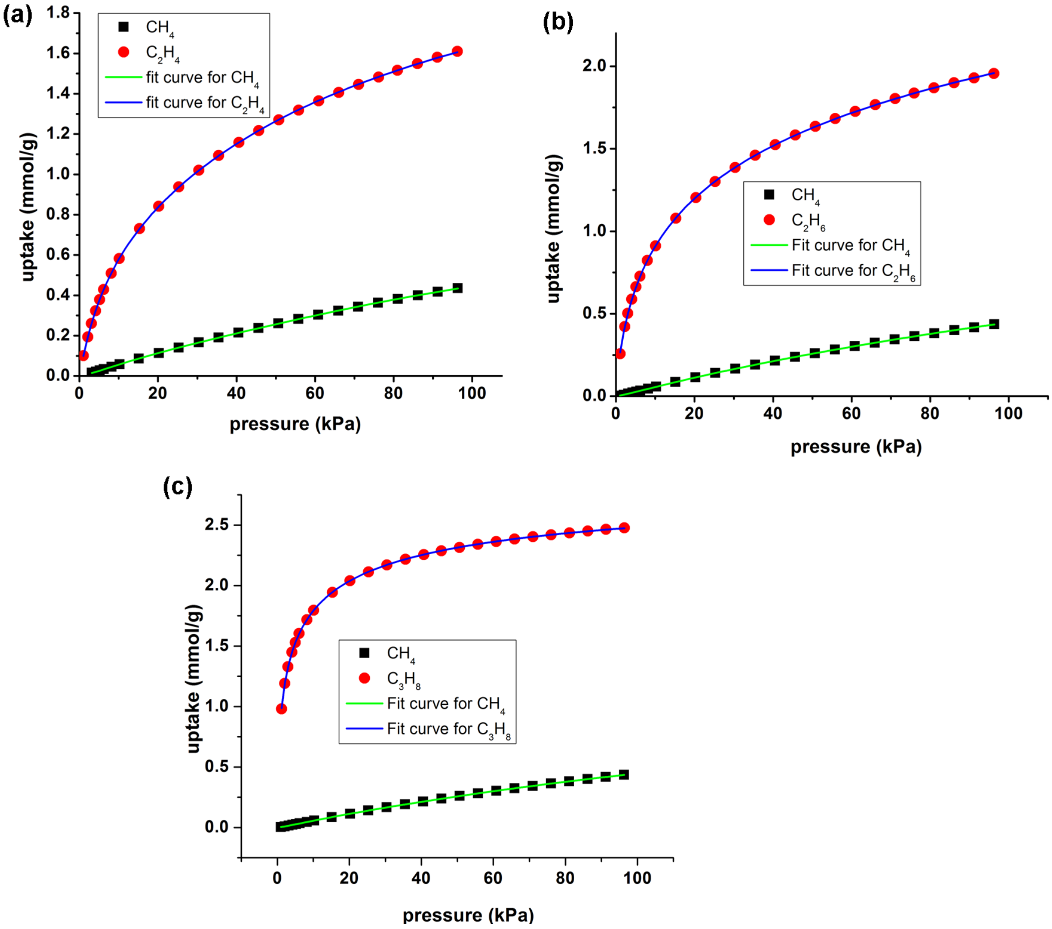

Figure S15. The adsorption isotherms of pure component gas (a) CH_4 and C_2H_4; (b) CH_4 and C_2H_6; (c) CH_4 and C_3H_8 for MCOF-1 at 298 K. Isotherms are fitted using the dual-site Langmuir-Freundlich equation.

Table S4. Comparison of C_2H_6/CH_4 and C_2H_4/CH_4 selectivity of MCOF with some other porous materials.

Material	C_2H_6/CH_4	C_2H_4/CH_4	References
MCOF-1	88	26	This work
UTSA-33a	16	12	S1
UTSA-34a	17	11	S1
UTSA-34b	22	18	S1
UTSA-35a	15	10	S2
La-PCP	22[a]	12[a]	S3
CuBTC	18	-	S4
MOF-505	16.30	-	S4
MgMOF-74	11.61	-	S4
CoMOF-74	7.77	-	S4
PCN-16	10.73	-	S4
mesoPOF-1	26	-	S5
mesoPOF-2	40	-	S5
mesoPOF-3	27.5	-	S5
ZJU-48a	8	-	S6

[a]. the selectivity is calculated using adsorption isotherm at 273 K.

References:

S1. Y. He, Z. Zhang, S. Xiang, H. Wu, F. R. Fronczek, W. Zhou, R. Krishna, M. O'Keeffe, B. Chen, *Chem.–Eur. J.*, 2012, **18**,1901.

S2. Y. He, Z. Zhang, S. Xiang, F. R. Fronczek, R. Krishna and B. Chen, *Chem. Commun.*, 2012, **48**, 6493.

S3. J. Duan, M. Higuchi, S. Horike, M. L. Foo, K. P. Rao, Y. Inubushi, T. Fukushima and S. Kitagawa, *Adv. Funct. Mater.* 2013, DOI: 10.1002/adfm.201203288.

S4. Y. He, R. Krishna, B. Chen, *Energy Environ. Sci.*, 2012, **5**, 9107.

S5. A. P. Katsoulidis, M. G. Kanatzidis, *Chem. Mater.*, 2012, **24**, 471.

S6. H. Xu, B. Chen G. Qian, J. Mater. Chem. A, 2013, DOI: 10.1039/C3TA12086D.